Controllable valley splitting in silicon quantum devices

SRIJIT GOSWAMI[1]*, K. A. SLINKER[1]*, MARK FRIESEN[1]*†, L. M. MCGUIRE[1], J. L. TRUITT[1], CHARLES TAHAN[2], L. J. KLEIN[1], J. O. CHU[3], P. M. MOONEY[4], D. W. VAN DER WEIDE[5], ROBERT JOYNT[1], S. N. COPPERSMITH[1] AND MARK A. ERIKSSON[1]†

[1]Department of Physics, University of Wisconsin-Madison, Wisconsin 53706, USA
[2]Cavendish Laboratory, J J Thomson Avenue, Cambridge CB3 0HE, UK
[3]IBM Research Division, T. J. Watson Research Center, New York 10598, USA
[4]Department of Physics, Simon Fraser University, Burnaby, British Columbia V5A 1S6, Canada
[5]Department of Electrical and Computer Engineering, University of Wisconsin-Madison, Wisconsin 53706, USA
*These authors contributed equally to this work
†e-mail: friesen@cae.wisc.edu; maeriksson@wisc.edu

Published online: 10 December 2006; doi:10.1038/nphys475

Silicon has many attractive properties for quantum computing, and the quantum-dot architecture is appealing because of its controllability and scalability. However, the multiple valleys in the silicon conduction band are potentially a serious source of decoherence for spin-based quantum-dot qubits. Only when a large energy splits these valleys do we obtain well-defined and long-lived spin states appropriate for quantum computing. Here, we show that the small valley splittings observed in previous experiments on Si–SiGe heterostructures result from atomic steps at the quantum-well interface. Lateral confinement in a quantum point contact limits the electron wavefunctions to several steps, and enhances the valley splitting substantially, up to 1.5 meV. The combination of electrostatic and magnetic confinement produces a valley splitting larger than the spin splitting, which is controllable over a wide range. These results improve the outlook for realizing spin qubits with long coherence times in silicon-based devices.

The fundamental unit of quantum information is the qubit. Qubits can be constructed from the quantum states of physical objects such as atomic ions[1], quantum dots[2–7] or superconducting Josephson junctions[8]. A key requirement is that these quantum states should be well defined and isolated from their environment. An assemblage of many qubits into a register and the construction of a universal set of operations, including initialization, measurement and single- and multiqubit gates, would enable a quantum computer to execute algorithms for certain difficult computational problems such as prime factorization and database search far faster than any conventional computer[9].

The solid state affords special benefits and challenges for qubit operation and quantum computation. State-of-the-art fabrication techniques enable the positioning of electrostatic gates with a resolution of several nanometres, paving the way for large-scale implementations. On the other hand, the solid-state environment provides numerous pathways for decoherence to degrade the computation[10]. Spins in silicon offer a special resilience against decoherence because of two desirable materials properties[11,12]: a small spin–orbit coupling and predominantly spin-zero nuclei. Isotopic purification could essentially eliminate all nuclear decoherence mechanisms.

Silicon, however, also has a property that potentially can increase decoherence. Silicon has multiple conduction-band minima or valleys at the same energy. Unless this degeneracy is lifted, coherence and qubit operation will be threatened. In strained-silicon quantum wells, there are two such degenerate valleys[13], whose quantum numbers and energy scales compete directly with the spin degrees of freedom. In principle, sharp confinement potentials, such as the quantum-well interfaces, couple these two valleys and lift the degeneracy, providing a unique ground state if the coupling is strong enough[14,15]. Theoretical analyses for non-interacting electrons in perfectly flat (100) quantum wells predict a valley splitting of the order of 1 meV or 10 K (ref. 15). However, existing data for Si–SiGe quantum wells, obtained so far at high magnetic fields, show a small valley splitting. Extrapolation to low fields suggests a valley splitting of only μeV, much too small for spintronics applications[16–20].

Here, we show that valley splitting can be controlled and greatly enhanced by confinement in nanostructures. Theoretically, we show that atomic steps at a quantum-well interface suppress the valley splitting compared with a flat interface. This suggests that lateral confinement would increase the valley splitting by reducing the number of steps seen by the wavefunction. We demonstrate experimentally that electronic confinement in nanostructures leads to very large valley splittings that approach the theoretical predictions for flat quantum wells with no steps[15]. At all magnetic fields, the valley splitting is much larger than the spin splitting, as required for quantum computing. We also probe the effects of magnetic confinement in the absence of electronic confinement by using a wide Hall bar geometry. A low-field microwave spectroscopy, analogous to electrically detected electron spin resonance[21], enables us to measure valley splitting in smaller magnetic fields than previously possible. In the absence of strong

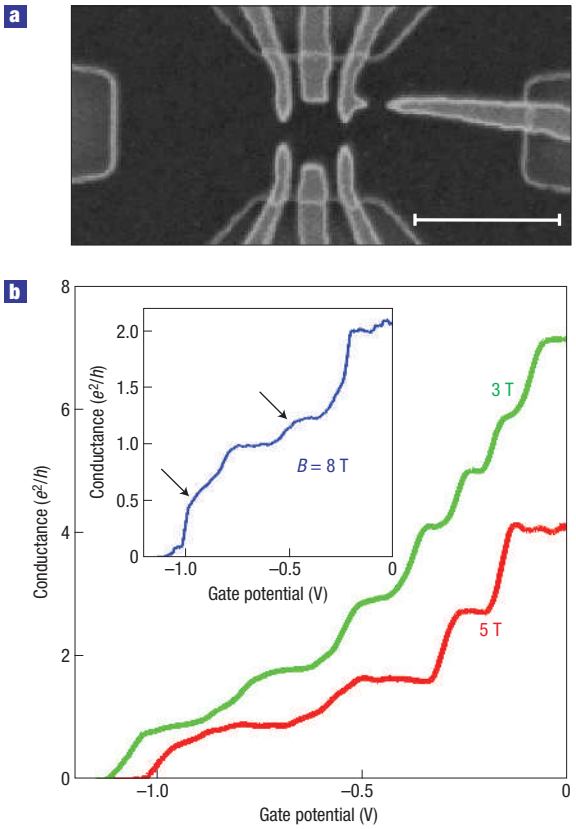

Figure 1 Quantum point contact. a, The experimental device used in the conduction measurements. The scale bar defines 1 μm. **b**, The conductance data as a function of gate voltage. Steps occur every e^2/h, indicating complete lifting of all degeneracies. At the magnetic field $B = 8$ T, the inset shows features reminiscent of the so-called 0.7 structure[34].

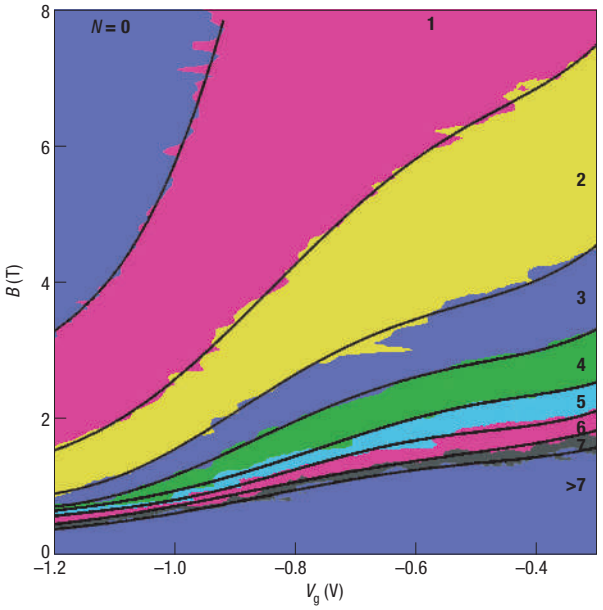

Figure 2 Step transitions. The step transitions between conductance plateaux in Fig. 1b are mapped out as a function of B and V_g. The dark lines show the results of fitting to equation (4), as described in the Supplementary Information.

lateral confinement, the valley splitting is less than the spin splitting and shows a strikingly linear dependence on magnetic field.

The key physical feature of our samples that is affected by confinement is the presence of steps in the quantum well. The Si–SiGe quantum wells used in all of our experiments were grown on a 2° tilt from (100), as is common in commercial wafers. (Further details on the sample growth are provided in the Methods section.) In addition to global tilt, strained heterostructures such as those used here also show natural roughness and local tilting. It has been suggested that valley splitting is strongly suppressed at quantum-well interfaces that are tilted with respect to their crystallographic axes[22], and we have developed an effective-mass theory to calculate the valley splitting in miscut quantum wells[23]. Our theory results in the following expression for the valley splitting:

$$E_v = 2\left|\int e^{-2ik_0 z}|F(\mathbf{r})|^2 V_v(\mathbf{r})\, d^3r\right|. \quad (1)$$

Here, $F(\mathbf{r})$ is a conventional envelope function oriented with respect to the tilted quantum well. The phase factor $e^{-2ik_0 z}$ arises from the Kohn–Luttinger effective-mass approximation[24], and is oriented with respect to the crystallographic axis, not the quantum well. Equation (1) can be understood as an overlap of the wavefunctions in k-space, which are centred on the valley minima $\pm k_0\hat{z}$. The valley coupling potential $V_v(\mathbf{r})$ is non-zero only within several ångströms of the quantum-well interface. We can approximate it as a Dirac δ-function:

$$V_v(\mathbf{r}) = v_0\delta(z - z_i(x)), \quad (2)$$

where v_0 is the strength of the valley coupling, and the interface position $z_i(x)$ describes the tilted plane of the quantum well. For quantum wells with no tilt, equations (1) and (2) agree very well with sophisticated tight-binding theories[15]. The theories predict oscillations of the valley splitting as a function of quantum-well width, due to different phase factors on the top and bottom interfaces. Such interference effects are a recurring theme in valley coupling[25], leading to the suppression of E_v.

Similar interference effects also lead to a strong suppression of the valley splitting in a tilted quantum well. To evaluate this effect, we treat the tilted interface as a series of atomic steps. In equation (1), the phase angles associated with consecutive steps differ by $\sim 0.85\pi$, and are nearly out of phase. For an electron spread over many steps, the valley splitting is strongly suppressed, and vanishes completely in the limit of full delocalization. However, under lateral confinement (for example, magnetic confinement), the electron covers only a finite number of steps, leading to an increased valley splitting compared with delocalized electrons. In the presence of an external confinement potential (for example, a quantum dot), the magnetic field and the external potential will both enhance valley splitting, with an approximate form given by

$$E_v \simeq \sqrt{\Delta_{ext}^2 + (\Delta_B B)^2}, \quad (3)$$

where Δ_{ext} is the valley splitting due to the external, electrostatic potential, Δ_B is the asymptotic slope of the valley splitting and B is the magnetic field.

Here, we describe our experiments in nanostructured devices in a two-dimensional electron gas (2DEG), demonstrating control of valley splitting by confinement. We first make use of the

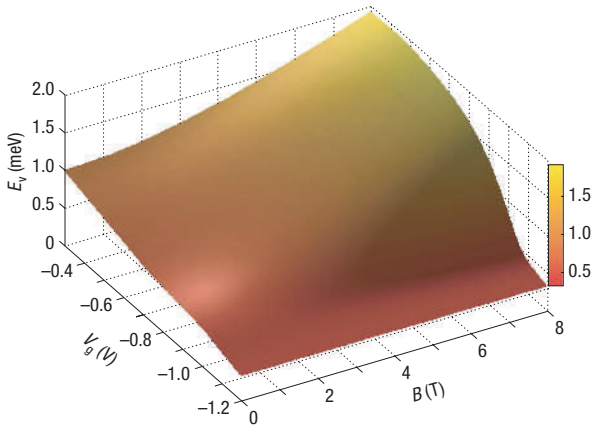

Figure 3 Valley splitting. A perspective plot of the valley splitting in the lowest quantum subband as a function of B and V_g. The splitting is large and can be controlled as a function of B and V_g.

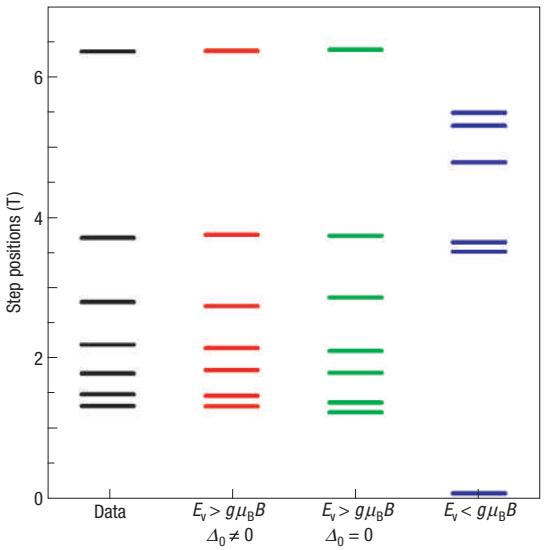

Figure 4 Comparison of valley and spin excitations. The experimental step transitions for $V_g = 0.5$ V in column 1 are compared with fits to equation (4) (columns 2–4) under differing constraints. Column 2 shows good agreement with the data when the valley splitting is constrained to be larger than the spin splitting. In contrast, column 4 shows poor agreement under the opposite constraint. Column 3 shows an alternative fit, with valley splitting larger than spin splitting, but vanishing at zero magnetic field.

device shown in Fig. 1a. By applying a negative bias to pairs of gates, we deplete the underlying 2DEG to form quantum point contacts[26]. Previous analyses have shown how to fit conductance data to a model hamiltonian and extract the orbital subband energy spacings, making use of the fact that the conductance in quantum point contacts is quantized in units of e^2/h multiplied by the number of occupied subbands[27]. Here, $-e$ is the electron charge, and h is Planck's constant.

In this work, we extend this approach and show that the valley splitting itself can be extracted from point-contact conductance characteristics. Figure 1b shows the quantized conductance through a point contact in the device shown. For nearly degenerate spin and valley states, we would expect conductance steps of four times the conductance quantum ($4e^2/h$). However, the steps clearly occur every e^2/h, indicating both non-zero spin and non-zero valley splittings. We analyse the point-contact spectroscopy data as follows. Building on equation (3), we write the subband energies of the quantum point contact as[27]

$$E_{\mathrm{QPC}} = (n+1)\sqrt{(\hbar\omega_0)^2 + (eB\hbar/2m^*)^2} + n_{\mathrm{B}} g \mu_{\mathrm{B}} B + n_{\mathrm{v}} E_{\mathrm{v}} + eV_{\mathrm{b}}, \quad (4)$$

where E_v is given in equation (3). The first term in equation (4) is the kinetic energy, where n denotes the subband index, $\hbar\omega_0$ is the electrostatic confinement energy and m^* is the transverse electron effective mass in silicon. The second term is the Zeeman spin splitting, and the fourth is the electrostatic potential. The third term is the valley splitting that we seek. The indices $n_B, n_v = \pm 1/2$ correspond to the Zeeman and valley states, respectively, $g \simeq 2$ is the electron g-factor and μ_B is the Bohr magneton. The electrostatic potential V_b depends on the gate voltage V_g but not on n. Because the size of the subband wavefunction determines the number of atomic steps that are covered, Δ_{ext} and Δ_{B} depend on both V_g and the subband index n. From equation (4), we see that E_{QPC} varies smoothly as a function of the gate voltage and the magnetic field. However, as V_g and B are varied, the number of modes below the Fermi level changes discretely, causing steps in conductance, as observed in Fig. 1b.

We have measured the quantum-point-contact conductance as a function of gate voltage and magnetic field (80 magnetic field traces, each at 700 different gate voltages), as shown in Fig. 2. To fit the transitions between conductance plateaux, we have mapped the experimental data to the nearest integer multiples of e^2/h, corresponding to the numerical labels shown[27], and have smoothed the transitions using higher-order polynomials (see the figure). As described in detail in the Supplementary Information, we fit to equation (4) and obtain Δ_{ext} and Δ_{B}, for $n = 1$ and $n = 2$, and V_b, all as a function of V_g and B. The confinement energy, $\hbar\omega_0$, was found to remain essentially constant and very small for all gate voltages. To help stabilize the fitting procedure, we fix ω_0 to zero.

The resulting valley splitting for the subband with $n = 1$ is plotted in Fig. 3, whereas the valley splitting for the subband with $n = 2$ is shown in the Supplementary Information. (Data from a second device on the same wafer, not shown, yield results that are very similar to those shown here.) The results show that the valley splitting is a tuneable function of both electrostatic and magnetic confinement. A crucial question is whether the valley splitting is larger than the spin splitting. We have carried out many variations of the analysis presented here. For example, equation (4) can be implemented with the valley splitting either larger or smaller than the spin splitting. Figure 4 shows the best fits obtained using valley splitting both larger and smaller than the spin splitting. The best fit with the valley splitting constrained to be smaller than the spin splitting is shown in the right-hand column, and it is very poor. Thus, we conclude that the valley splitting is larger than the spin splitting in our quantum point contacts. A more subtle question involves the precise form of equation (4). For example, could the valley splitting be zero at zero applied magnetic field? As shown in Fig. 4, the fit with a non-zero intercept is better than the fit with a zero intercept, but not dramatically so. Thus, we are confident that the valley splitting is larger than the spin splitting for even arbitrarily small magnetic fields, but we cannot say with complete confidence that the valley splitting is non-zero at zero magnetic field.

The valley splitting shows an interesting dependence on gate voltage as well as on magnetic field, decreasing as the device

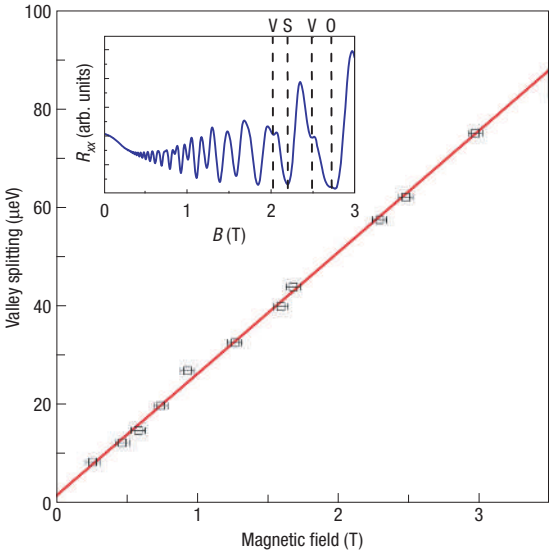

Figure 5 Microwave spectroscopy of the valley splitting in a Si–SiGe Hall bar. The inset shows Shubnikov–de Haas oscillations, with the valley (V), spin (S) and orbital (O) minima labelled. Magnetic confinement causes the valley splitting to increase as the magnetic field increases. The error bars reflect small shifts in the peak positions with varying microwave power.

moves closer to pinch-off. Near pinch-off, the electron density is low, so many-body enhancements to the valley splitting are negligible. We therefore compare the experimentally measured valley splitting at pinch-off (~0.35 meV) with the predictions of single-electron theory. As described in the Supplementary Information, the resulting prediction for our quantum point contact is $E_v = 0.46$ meV; because the magnetic confinement is weaker than the electrostatic confinement, the valley splitting is independent of magnetic field. The fact that the experimental measurement is slightly smaller than the theoretical value suggests that the few-electron limit is appropriate, but that the presence of several interfacial steps may suppress the valley splitting slightly compared with a flat well. In other regions of Fig. 3, where the electron density is larger, the valley splitting is larger than the theoretical prediction for non-interacting electrons, and it shows a significant magnetic-field dependence. We ascribe this behaviour to many-body effects, which have been considered elsewhere[28], but are not yet fully understood.

Our measurements of the valley splitting in a quantum point contact seem to be consistent with the few-electron, few-step limit. The same conclusions should therefore also apply to a small-quantum-dot geometry. We expect a quantum dot fabricated in an equivalent quantum well to produce a valley splitting in the range 0.35–0.46 meV, depending on the size of the dot. Additional control of the valley splitting can be achieved by varying the quantum-well width or the doping density. The former has a very strong effect on the valley splitting, but can also lead to valley-splitting oscillations[15]. The latter essentially determine the electric field on the quantum dot. We believe the doping density forms a more robust design parameter, and may lead to valley splittings of the order of 1 meV. Additional details and discussion are provided in the Supplementary Information.

Finally, we probe the limit of weak lateral confinement, using a Hall bar geometry. As shown in the inset of Fig. 5, Shubnikov–de Haas oscillations in a 2DEG reveal the lifting of both the spin and valley degeneracies at high magnetic field. Previous results indicate that the valley splitting is smaller than the spin splitting in large structures such as this Hall bar[16–20], a result that we confirm here with microwave spectroscopy.

Microwave-driven electron spin resonance can be detected by measuring the change in resistance of a Hall bar on application of a microwave field[29], so-called electrically detected electron spin resonance. We have carried out electrically detected electron spin resonance and observed the classic Zeeman spin splitting with a g-factor of two, as expected for silicon. Here we extend this technique and use microwave spectroscopy to measure the valley splitting. The valley splitting values E_v are smaller than the spin splitting, and are presented in Fig. 5 as a function of the applied magnetic field. The smaller magnitude of the valley splitting explains the weaker minima in the Shubnikov–de Haas oscillations associated with the valley splitting. The microwave spectroscopy shows that the valley splitting is linear all the way down to 0.3 T, with a slope of $24.7 \pm 0.4\,\mu\text{eV T}^{-1}$. The sharpness of the resonance peaks allows very tight error bars, with a small zero-field intercept of $E_v(0) = 1.5 \pm 0.6\,\mu\text{eV}$. The slope and intercept are in general agreement with previous reports in Si–SiGe quantum wells[16] and Si inversion layers[18], but the present work extends these measurements down to much lower fields.

Qualitatively, the magnetic-field dependence of the 2DEG data is consistent with the theory discussed above. In a magnetic field, the electron is confined over the magnetic length scale $l_B = \sqrt{\hbar/|eB|}$. Numerical investigations of the valley splitting in a stepped quantum well yield trends similar to Fig. 5, with valley splitting increasing as B increases. To obtain correspondence with the data, we must introduce specific, though plausible, disorder models for the step profiles. The simulations then predict slopes very similar to our valley resonance experiments, and a valley splitting that essentially vanishes at zero field.

We have shown here that valley splitting can be controlled through both physical and magnetic confinement. The small valley splitting observed in numerous previous experiments arises because disorder and steps in the quantum well suppress the valley splitting by interference. As a consequence, strong lateral confinement can reduce the interference and increase valley splitting substantially. It is interesting to note that these results now point to other ways of increasing the valley splitting. For example, a smaller step density can be obtained by growing on substrates with little average tilt (for example, in certain Si–SiO_2 devices[30]). However, the thick growths required to obtain relaxed SiGe on Si substrates will still lead to steps arising from dislocation formation. An alternative that requires no dislocations is the growth of 2DEGs in Si–SiGe nanomembranes[31]. More generally, these results show that even properties that at first glance seem to be intrinsic and unalterable—in large part a band-structure phenomenon—can in fact be tuned and controlled with methods of nanoscale fabrication.

METHODS

MATERIALS GROWTH

The Si–SiGe heterostructures used in these experiments were grown by ultrahigh-vacuum chemical vapour deposition[32]. For each sample, the 2DEG is located in a strained Si quantum well grown on a strain-relaxed $Si_{1-x}Ge_x$ buffer layer. For the quantum-point-contact experiment, $x = 0.25$, the quantum-well width is 100 Å, and the density and mobility are $n = 5.7 \times 10^{11}\ \text{cm}^{-2}$ and $\mu = 200{,}000\ \text{cm}^2\ \text{V}^{-1}\ \text{s}^{-1}$, respectively. For the sample used in the microwave measurements, $x = 0.3$, the quantum-well width is 80 Å, the 2DEG density $n = 4.2 \times 10^{11}\ \text{cm}^{-2}$ and the mobility $\mu = 40{,}000\ \text{cm}^2\ \text{V}^{-1}\ \text{s}^{-1}$. Further details of the structures can be found in ref. 33.

Received 21 July 2006; accepted 3 November 2006; published 10 December 2006.

References

1. Cirac, J. & Zoller, P. Quantum computations with cold trapped ions. *Phys. Rev. Lett.* **74**, 4091–4094 (1995).
2. Loss, D. & DiVincenzo, D. P. Quantum computation with quantum dots. *Phys. Rev. A* **57**, 120–126 (1998).
3. Ciorga, M. *et al.* Addition spectrum of a lateral dot from Coulomb and spin-blockade spectroscopy. *Phys. Rev. B* **61**, R16315–R16318 (2000).
4. Fujisawa, T., Austing, D. G., Tokura, Y., Hirayama, Y. & Tarucha, S. Allowed and forbidden transitions in artificial hydrogen and helium atoms. *Nature* **419**, 278–281 (2002).
5. Elzerman, J. M. *et al.* Single-shot read-out of an individual electron spin in a quantum dot. *Nature* **430**, 431–435 (2004).
6. Johnson, A. C. *et al.* Tripletsinglet spin relaxation via nuclei in a double quantum dot. *Nature* **435**, 925–928 (2005).
7. Petta, J. R. *et al.* Coherent manipulation of coupled electron spins in semiconductor quantum dots. *Science* **309**, 2180–2184 (2005).
8. Shnirman, A., Schön, G. & Hermon, Z. Quantum manipulations of small Josephson junctions. *Phys. Rev. Lett.* **79**, 2371–2374 (1997).
9. Nielsen, M. & Chuang, I. *Quantum Computation and Quantum Information* (Cambridge Univ. Press, Cambridge, 2000).
10. Cerletti, V., Coish, W. A., Gywat, O. & Loss, D. Recipes for spin-based quantum computing. *Nanotechnology* **16**, R27–R49 (2005).
11. Kane, B. E. A silicon-based nuclear spin quantum computer. *Nature* **393**, 133–137 (1998).
12. Yablonovitch, E. *et al.* Optoelectronic quantum telecommunications based on spins in semiconductors. *Proc. IEEE* **91**, 761–780 (2003).
13. Schäffler, F. High-mobility Si and Ge structures. *Semicond. Sci. Technol.* **12**, 1515–1549 (1997).
14. Ando, T., Fowler, A. B. & Stern, F. Electronic properties of two-dimensional systems. *Rev. Mod. Phys.* **54**, 437–672 (1982).
15. Boykin, T. B. *et al.* Valley splitting in strained silicon quantum wells. *Appl. Phys. Lett.* **84**, 115–117 (2004).
16. Weitz, P., Haug, R. J., von Klitzing, K. & Schäffler, F. Tilted magnetic field studies of spin- and valley-splittings in Si/$Si_{1-x}Ge_x$ heterostructures. *Surf. Sci.* **361/362**, 542–546 (1996).
17. Koester, S. J., Ismail, K. & Chu, J. O. Determination of spin- and valley-split energy levels in strained Si quantum wells. *Semicond. Sci. Technol.* **12**, 384–388 (1997).
18. Khrapai, V. S., Shashkin, A. A. & Dolgopolov, V. P. Strong enhancement of the valley splitting in a two-dimensional electron system in silicon. *Phys. Rev. B* **67**, 113305 (2003).
19. Lai, K. *et al.* Two-flux composite fermion series of the fractional quantum Hall states in strained Si. *Phys. Rev. Lett.* **93**, 156805 (2004).
20. Pudalov, V. M., Punnoose, A., Brunthaler, G., Prinz, A. & Bauer, G. Valley splitting in Si-inversion layers at low magnetic fields. Preprint at <http://arxiv.org/abs/cond-mat/0104347> (2001).
21. Dobers, M., von Klitzing, K., Schneider, J., Weimann, G. & Ploog, K. Electrical detection of nuclear magnetic resonance in GaAs−$Al_xGa_{1-x}As$ heterostructures. *Phys. Rev. Lett.* **61**, 1650–1653 (1988).
22. Ando, T. Valley splitting in the silicon inversion layer: Misorientation effects. *Phys. Rev. B* **19**, 3089–3095 (1979).
23. Friesen, M., Eriksson, M. A. & Coppersmith, S. N. Magnetic field dependence of valley splitting in realistic Si/SiGe quantum wells. *Appl. Phys. Lett.* **89**, 202106 (2006).
24. Kohn, W. in *Solid State Physics* Vol. 5 (eds Seitz, F. & Turnbull, D.) 257–319 (Academic, New York, 1957).
25. Koiller, B., Hu, X. & das Sarma, S. Exchange in silicon-based quantum computer architecture. *Phys. Rev. Lett.* **88**, 027903 (2002).
26. Van Wees, B. J. *et al.* Quantized conductance of point contacts in a two-dimensional electron gas. *Phys. Rev. Lett.* **60**, 848–850 (1988).
27. Van Wees, B. J. *et al.* Quantum ballistic and adiabatic electron transport studied with quantum point contacts. *Phys. Rev. B* **43**, 12431–12453 (1991).
28. Ohkawa, F. J. & Uemura, Y. Theory of valley splitting in an *N*-channel (100) inversion layer of Si III. Enhancement of splittings by many-body effects. *J. Phys. Soc. Jpn* **43**, 925–932 (1977).
29. Jiang, H. W. & Yablonovitch, E. Gate-controlled electron spin resonance in GaAs/$Al_xGa_{1-x}As$ heterostructures. *Phys. Rev. B* **64**, 041307 (2001).
30. Takashina, K., Ono, Y., Fujiwara, A., Takahashi, Y. & Hirayama, Y. Valley polarization in Si(100) at zero magnetic field. *Phys. Rev. Lett.* **96**, 236801 (2006).
31. Roberts, M. M. *et al.* Elastically relaxed free-standing strained-silicon nanomembranes. *Nature Mater.* **5**, 388–393 (2006).
32. Ismail, K., Arafa, M., Saenger, K. L., Chu, J. O. & Meyerson, B. S. Extremely high electron mobility in Si/SiGe modulation-doped heterostructures. *Appl. Phys. Lett.* **66**, 1077–1079 (1995).
33. Klein, L. J. *et al.* Coulomb blockade in a silicon/silicon-germanium two-dimensional electron gas quantum dot. *Appl. Phys. Lett.* **84**, 4047–4049 (2004).
34. Cronenwett, S. M. *et al.* Low-temperature fate of the 0. 7 structure in a point contact: A Kondo-like correlated state in an open system. *Phys. Rev. Lett.* **88**, 226805 (2002).

Acknowledgements

We gratefully acknowledge conversations with R. Blick. This work was supported by NSA/LPS under ARO contract number W911NF-04-1-0389, and by the National Science Foundation through the ITR programme (DMR-0325634) and the EMT programme (CCF-0523675).
Correspondence and requests for materials should be addressed to M.F. or M.A.E.
Supplementary Information accompanies this paper on www.nature.com/naturephysics.

Author contributions

J.C. and P.M. provided the samples. S.G., K.S., L.M., J.T., and L.K. carried out the fabrication and measurements. M.F., C.T., R.J. and S.C. did the theoretical work. S.G., K.S., L.M., M.F., S.C. and M.E. analysed the data. M.F., R.J., D.W., S.C., M.F. and M.E. planned the project. M.F., K.S., S.C. and M.E. prepared the manuscript.

Competing financial interests

The authors declare that they have no competing financial interests.